Effects of Nonlinearities in Black Box Identification of an Industrial Robot

Martin Aberger

Department of Electrical Engineering
Linköping University, SE-581 83 Linköping, Sweden
WWW: http://www.control.isy.liu.se
Email: marab709@student.liu.se

December 11, 2000



Report no.: LiTH-ISY-R-2322

Technical reports from the Automatic Control group in Linköping are available by anonymous ftp at the address ftp.control.isy.liu.se. This report is contained in the file 2322.pdf.

Effects of Nonlinearities in Black Box Identification of an Industrial Robot

Martin Aberger*
Department of Electrical Engineering
Linköping University, SE-58 183 Linköping, Sweden
Email: marab709@student.liu.se

December 11, 2000

Abstract

This paper discusses effects of nonlinearities in black box identification of one axis of a robot. The used data come from a commercial ABB robot, IRB1400. A three-mass flexible model for the robot was built in MathModelica. The nonlinearities in the model are nonlinear friction and backlash in the gear box.

1 Introduction

In this report we are looking at the effects of nonlinearities in black box identification of one axis of a robot. We built a model of the robot in *MathModelica* and then we used the simulated data in *Matlab* for the identification [2]. The data that we use come from a commercial six degrees of freedom ABB robot, IRB1400. We are only moving axis one, that is the motor in the bottom. All other motors are not moving. For the model of the arm of the robot we are using a three-mass flexible model as an approximation, as shown in Figure 1. The notations for the model are shown in Table 1.

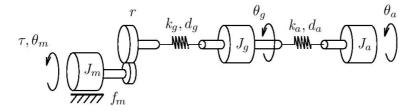


Figure 1: Three-mass flexible model.

The first mass represents the rotating part of the electrical motor, and it is followed by a gear box. The flexibility in the gear box is in the model represented

^{*}On leave from Johannes Kepler Universität Linz, A-4040 Linz, Austria.

| θ_m | motor angle |
|------------|---|
| θ_a | arm angle |
| J_m | moment of inertia of the motor |
| J_a | moment of inertia of the arm |
| J_g | moment of inertia of the gear box |
| f_m | friction coefficient of the motor |
| k_g | spring constant of the gear box |
| k_a | spring constant of the arm |
| τ | motor torque |
| d_g | damping coefficient in spring of the gear box |
| d_a | damping coefficient in spring of the arm |
| r | gear box ratio $(\frac{1}{118})$ |

Table 1: Notations.

| $J_m (10^{-4})$ | J_g | J_a | $f_m (10^{-2})$ | $k_g (10^5)$ | $k_a (10^5)$ | d_g | d_a |
|-----------------|-------|-------|-----------------|--------------|--------------|-------|-------|
| 4.56 | 9.92 | 1.72 | 3.55 | 1.50 | 0.446 | -62 | 20 |

Table 2: Physical parameters or the linear model.

by the spring and the damper between the gear box and the second mass. The second spring and damper represents the flexibility in the robot arm. Torque balances for the three masses yield to the following equations:

$$\tau = J_m \ddot{\theta}_m + \tau_{Friction} + r \cdot d_g \left(r \dot{\theta}_m - \dot{\theta}_g \right) + r \cdot k_g \left(r \theta_m - \theta_g \right) \tag{1}$$

$$0 = J_g \ddot{\theta}_g - d_g \left(r\dot{\theta}_m - \dot{\theta}_g \right) - k_g \left(r\theta_m - \theta_g \right) + d_a \left(\dot{\theta}_g - \dot{\theta}_a \right) + k_a \left(\theta_g - \theta_a \right) \quad (2)$$

$$0 = J_a \ddot{\theta}_a - d_a \left(\dot{\theta}_g - \dot{\theta}_a \right) - k_a \left(\theta_g - \theta_a \right) \tag{3}$$

The first attempt for the friction is a viscous friction and it is computed via $\tau_{Friction} = f_m \cdot \theta_m$. The parameters for the model are shown in Table 2. These parameters are from earlier identification of the robot [4].

The model in *MathModelica* is shown in Figure 2 [3]. For the linear model the backlash of the gear box is zero and there is no coulomb friction in the component *Friction* implemented.



Figure 2: MathModelica three-mass flexible model.

The input signal that we have chosen for the model is the same as for the identification of the parameters of the linear model. It is a chirp signal [0.5 Hz 30 Hz] with constant amplitude. The motor velocity is used as output signal. The sampling rate is 2000 Hz and then down-sampling with a factor of ten was done. The sample time for the simulation was therefore 5 ms. The measured input signal (motor torque τ) and the output signal (motor velocity θ_m) can be found in Figure 3.

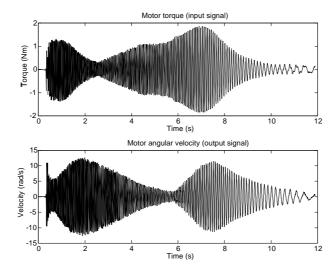


Figure 3: Input and output signal of the linear model.

For the black box identification we have chosen to work with Box-Jenkins models. Box-Jenkins models can be described, see [1], by

$$y(t) = \frac{B(q)}{F(q)}u(t) + \frac{C(q)}{D(q)}e(t)$$

$$(4)$$

where $B\left(q\right),\ C\left(q\right),\ D\left(q\right)$ and $F\left(q\right)$ are parameterized polynomials, u(t) is the input and e(t) is the noise. We have chosen a order of five and a time delay of one for the identification. Before the identification in Matlab could be done it was necessary to low-pass filter the simulated data. The data was filtered with $0.4 \cdot \omega_N \approx 251 \frac{\rm rad}{\rm s}$ where ω_N is the Nyquist frequency. The order of the filter we used was eight.

2 Black Box Identification of the linear model

The difference in the Bode plot of the Box-Jenkins model of the robot and the Box-Jenkins model of the simulated model is shown in Figure 4.

There is only a small difference for lower frequencies. The frequency for the second peak and for the second notch is lower for the Box-Jenkins model of the simulated model. The difference in the phase plot is a result of the negative damping coefficient.

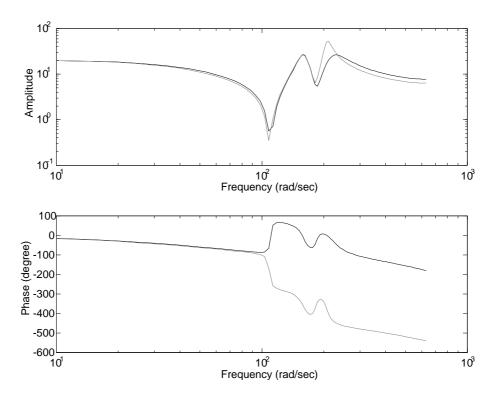


Figure 4: Bode plot of Box-Jenkins models. The model of the messured data from the robot in black and the model of the simulated robot in grey.

3 Black Box Identification of the Model with Coulomb Friction

The torque in the friction is defined in three different linear examples. We used always the same viscous friction coefficient from the identification.

linear case: $\tau_{Friction} = f_m \cdot \theta_m$ case 1: $\tau_{Friction} = 0.0355 \cdot \mathrm{sign}(\theta_m) + f_m \cdot \theta_m$ case 2: $\tau_{Friction} = 0.1 \cdot \mathrm{sign}(\theta_m) + f_m \cdot \theta_m$ case 3: $\tau_{Friction} = 0.355 \cdot \mathrm{sign}(\theta_m) + f_m \cdot \theta_m$

The difference in the Bode plot of the Box-Jenkins models with coulomb friction is shown in Figure 5.

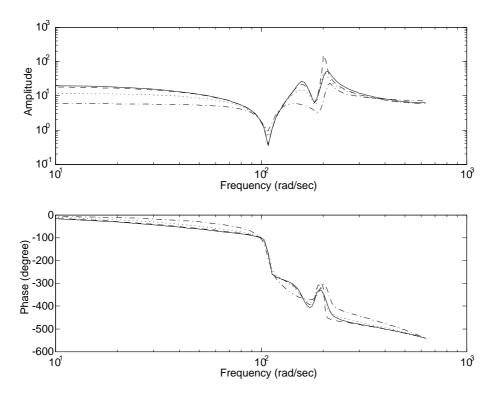


Figure 5: Bode plot of Box-Jenkins models. Linear model solid line, case 1 dashed line, case 2 dotted line and case 3 is shown with a dash dotted line.

The amplitude in the Bode plot is for lower frequencies decreasing when the coulomb friction is higher. The frequency of the first notch and the first peak is not changing with the implementation of a coulomb friction. The frequency of the second notch and the second peak is higher in case 4 than in the linear case. The frequency for the second peak is for small coulomb friction (case 1 and 2) a bit lower. Interesting is that the amplitude of the second peak for case 1 is much higher than in the linear case.

When the absolute angular velocity in the friction becomes zero, the friction becomes stuck, i.e., the absolute angle remains constant. The elements begin to

slide when the friction torque exceeds a threshold value, called the maximum static friction torque, computed via:

$$\tau_{static\ max} = peak \cdot \tau_{sliding} (\omega = 0)$$
 (5)

$$peak \ge 1 \tag{6}$$

 $\tau_{sliding} (\omega = 0)$ is the viscous friction torque at zero velocity.

The effect in the Box-Jenkins models of this static friction is shown in Figure 6.

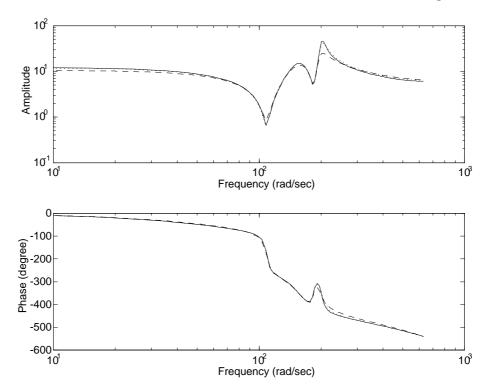


Figure 6: Bode plot of Box-Jenkins models. Case 2 with peak = 1 solid line, case 2 with peak = 2 dotted line and case 2 with peak = 5 dashed line.

The effect when implementing a maximum-static-friction in the Bode plot is for peak=2 very small. When the peak=5 the amplitude of the second peak is lower.

4 Black Box Identification of the Model with Backlash in the Gear Box

The effect in the Bode plot of the Box-Jenkins models with different total backlash b in the gear box is shown in Figure 7. The backlash is given in radians on the arm side.

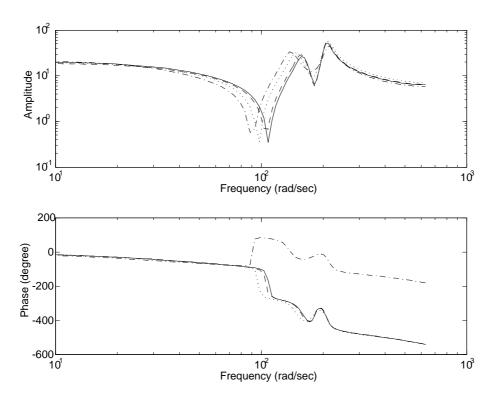


Figure 7: Bode plot of the Box-Jenkins models. Solid line no backlash, dashed line $b=0.0001\,\mathrm{rad}$, dotted line $b=0.0005\,\mathrm{rad}$, dashed dotted line $b=0.001\,\mathrm{rad}$.

The frequency of the first and second notch and the first peak in the Bode plot is lower with a higher backlash. There is no difference in the frequency for the second peak. It is also interesting that if the backlash is bigger then the phase in the Bode plot is becoming positive.

We have also reduced the input torque to 50% and 20% of the original input torque. The effect of this reduction in the Bode plot of the Box-Jenkins models is shown in Figure 8.

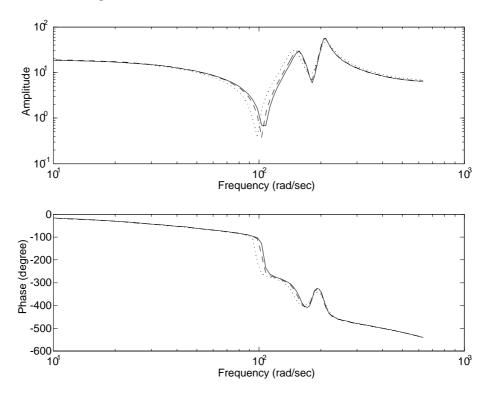


Figure 8: Bode plot of the Box-Jenkins models with backlash $b=0.0001\,\mathrm{rad}$. Solid line original input data, dashed line 50% input torque, dotted line 20% input torque.

The effect in the Bode plot is the same when you increase the backlash with the original input torque and when you decrease the input torque for a fixed backlash. The frequency of the first and second notch and the first peak in the Bode plot is lower when the input torque is lower. There is no difference in the frequency for the second peak. There is hardly any difference in the Bode plot of the model with backlash $b=0.0005\,\mathrm{rad}$ with original input torque and the model with backlash $b=0.0001\,\mathrm{rad}$ and 20% input torque.

5 Conclusions

We have presented Bode plots of black box identification of a simulated model of a robot arm with different kind of nonlinearities. The nonlinearities we introduced have been sometimes quit big to see the effect in the identification better. The basic characteristics of the black-box models do not change if we introduce nonlinearites. The backlash has a influence on the frequencies of the two notches and the first peak while the friction affects the amplitude over the whole frequency range and the frequency of the second peak.

References

- [1] L. Ljung. System Identification: Theory for the User. Prentice-Hall, Upper Saddle River, N.J. USA, 2:nd edition, 1999.
- [2] The MathWorks, Inc. System Identification Toolbox Version 4.0.5 (R11)
- [3] M. Otter. Free Modelica Standard Libraries. http://www.modelica.org/library/library.html.
- [4] M. Östring. Closed Loop Identification of the Physical Parameters of an Industrial Robot. Technical Report LiTH-ISY-R-2303, Department of Electrical Engineering, Linköping University, 2000.